Title
Optimal Preview Control For Vehicle Lateral Guidance

Authors
Peng, Huei
Tomizuka, Masayoshi

Publication Date
1991

CALIFORNIA 'PATH PROGRAM
INSTITUTE OF TRANSPORTATION STUDIES
UNIVERSITY OF CALIFORNIA AT BERKELEY

Optimal Preview Control for Vehicle Lateral Guidance

Huei Peng
Masayoshi Tomizuka

PATH Research Report
UCB-ITS-PRR-91-16

This work was performed as part of the California PATH Program of the University of California, in cooperation with the State of California, Business and Transportation Agency, Department of Transportation, and the United States Department of Transportation, Federal Highway Administration.

August 199 1

ISSN 10551425

Optimal Preview Control for Vehicle Lateral Guidance

Huei Peng and Masayoshi Tomizuka

August 31, 1991

Abstract

The *continuous time deterministic optimal preview control algorithm* is applied to lateral guidance of a vehicle for an automated highway. When a human driver steers a vehicle, his ability to look ahead (preview) the upcoming road, is crucial to control the vehicle so that it remains in the center of the lane, especially at sharp corners and winding sections. In this report, an *optimal preview control algorithm* is introduced which utilizes the preview information pertaining to road curvature as well as superelevation angle for vehicle lateral control purposes. The optimal control law consists of both feedback control action and feedforward preview control action. The feedforward preview control action significantly improves the tracking performance while maintaining a small closed loop bandwidth so that the ride quality is not impaired. Frequency-domain analyses and numerical simulation results show the improvements obtained in both the frequency domain and the time domain.

1. Introduction

The lateral control of vehicles is a critical component in highway automation. The objectives are 1) to steer the wheels intelligently so that the vehicle tracks the center of a lane with small error and 2) to maintain good ride quality under different vehicle speeds, loads, wind gust disturbances, and road surface conditions.

In [1], the feedback control algorithm was designed by utilizing the Frequency-Shaped Linear Quadratic (FSLQ) control theory [2][3], which allows the frequency-dependent ride quality to be included explicitly in the performance index. The high-frequency robustness of the control system can be ensured by properly choosing the weighting factors in the performance index. In [1], two different mathematical models were used to represent the lateral dynamics of a front-wheel-steered, rubber-tired vehicle. A simple linear model, which includes only lateral and yaw motions, was used to design the feedback and feedforward control laws. A more complicated nonlinear model, which includes the motion of the vehicle mass center in all six degrees of freedom plus suspension deflections and wheel motions, was used to evaluate the performance of controllers (refer to [1] for details on the vehicle models).

A feedforward compensator is used in [1] to improve the tracking performance when the vehicle is entering or leaving a curve. It is assumed that the compensator can make use of the current road curvature -information as well as the vehicle mass, velocity, and tire cornering stiffness to calculate the corresponding steady-state feedforward steering angle. The assumption that current road curvature information is available is extended so that the curvature information is available before the vehicle reaches the curved section, that is, as preview information. In this paper, the preview control algorithm, which utilizes this information, is presented. In addition, its effectiveness on the improvement of the tracking performance, especially at tight curved sections of the road, is examined by simulations.

Utilization of information related to the upcoming road characteristics is an important factor in vehicle lateral control. Roland and Sheridan [4] stressed the importance of preview information for the human driver, and simulated the drivers' response when the upcoming road suddenly changes. McRuer *et al.* [5] proposed that the human driver's control algorithm in performing a regulation task (lane following) consists of two parts: the pursuit (open-loop) block and the compensatory (closed loop) block. They concluded that the "pursuit" part in the human control system, which previews the future desired path, generates the major part of the driver commands, while the closed loop portion of the system merely reduces the residue errors. McLean and Hoffmann [6] conducted spectral analysis on the steering wheel motion of a human driver. The result agrees with McRuer's model, where two peaks occur in the spectral density: a primary peak, which coincides with the dominant frequency of the road being followed, and a secondary peak, which corresponds to the closed loop compensation motions of the driver. A list of possible visual cues used by human drivers for the pursuit (preview) control action was compiled in [7]; they include the vehicle heading angle (and rate), the vehicle path angle (and rate), and the time-advanced lateral

deviation, which is the vehicle displacement at a preview distance. McLean and Hoffmann [8] performed 'cross-correlation analysis and suggested that the vehicle heading angle was the dominant variable closely controlled by the human driver under normal driving conditions. When a severely restricted preview length is imposed on the driver, the heading rate of the vehicle becomes the major controlled variable.

Godthelp [9] presented a necessary feedfonvard steering angle for a particular (step-changed) road curve. This feedforward steering angle gradually ramps up to and down from a steady state value corresponding to the radius of curvature. The control law suggested by Kondo and Ajimine [10] and Liu and Frank [11] did not include a feed-forward part. Nevertheless, in their controllers the error signals for feedback control, which were the lateral deviation of the driver's sight [10] and the heading angle error to a future reference point [11] implicitly included preview information.

The optimal preview control for lateral guidance of vehicles has been studied by Lee [12] from the viewpoint of the discrete time preview control theory [13] [14]. In this paper, analysis and design of the preview controller is performed in the continuous time domain. In the optimal preview control, the road curvature over a finite preview segment [t, $t+t_{la}$] is assumed to be known; where t is the present time and t_{la} is the preview time. The road curvature beyond the preview segment is assumed to die out smoothly with known dynamics.

The road superelevation angle may have significant adverse effects on the lateral control of vehicles if it is not included in the model. It is suggested that the road superelevation angle be combined with the road curvature to form an "effective curvature" for control purposes. The "effective curvature" replaces the original road curvature in the preview control law. If the information on superelevation is not available, a large error may occur in the estimation of the average tire cornering stiffness (C_α), which deteriorates the tracking performance of the controller indirectly.

It should be noted that if the control algorithms in [10] and [11] are to be implemented, special on-board look-ahead sensors will be required. The preview information required for the control algorithm presented in this paper pertains to road curvature and superelevation, which can be measured from the road geometry or obtained from transportation agencies. These information can be retrieved from an on-board database, read from the discrete magnetic reference markers [15], or transmitted from the road to vehicles by any available means. Therefore, the present preview control approach is more practical to implement.

The transfer functions from disturbance (road curvature) to lateral tracking error and lateral acceleration under preview control are derived from the linear model. Frequency domain analysis of the preview control algorithm is performed. This analysis shows that the preview action reduces the lateral tracking error in the low frequency region significantly. Furthermore, the steering action under preview control is initiated before the road curvature starts to change, and is smooth throughout the curved

section. As a consequence, the lateral acceleration in the high frequency region is also reduced.

A numerical simulation study is performed by using the complex vehicle model to demonstrate the improvement achieved by the preview controller. Simulations are performed for selected values of preview time, vehicle speed, road surface condition, curvature and superelevation. The gain scheduling technique is used to tune the feedback and feedforward gain matrices for varying vehicle speeds and road surface conditions (see [1] for details). Intermittent measurement of the lateral tracking error is emphasized to ensure that the magnetic marker scheme developed for the PATH program [15] works well with the preview controller. Simulation results show that the preview controller is promising and performs well under all the above stated conditions.

2. Feedback/Feedforward/Preview Control

The optimal preview control problems have been studied extensively throughout the 60's and 70's [16]-[19] in various applications. They can be categorized into two types depending on the "previewed signal": either the desired trajectory in a tracking problem, or the external disturbance signal in a regulating problem. Based on the amount of information on reference inputs and/or disturbances available to the controller, the control problem may be categorized into three types (see Figure 1): the pure feedback control problem, the feedback/feedforward control problem, and the feedback/preview control problem. When none of the future information (either desired trajectory or disturbance signal) is available, and the control signal is calculated solely based on the error signal, it is a feedback control problem. When the controller utilizes the current desired trajectory (or disturbance) signal as well as the error signal, we have feedback/feedforward control. When the future information is available and utilized by the control law, we have feedback/preview control. An extensive development of preview control for tracking problems can be found in [20], and that for regulation problems can be found in [21]. The optimal finite preview problem is presented in this paper and applied to the vehicle lateral guidance problem, where the road curvature and road superelevation enter the system dynamic equation as external disturbances, and are assumed to be previewable. The following points should be noted:

(1) In this report, the problem is studied from a deterministic point of view. That is, the road curvature is obtained without any measurement noises, although quantization error may exist.

(2) The preview time is assumed to be finite. That is, at time t, the road curvature in $\tau \in [t, t+t_{la}]$ is assumed to be known, where t_{la} is the preview time.

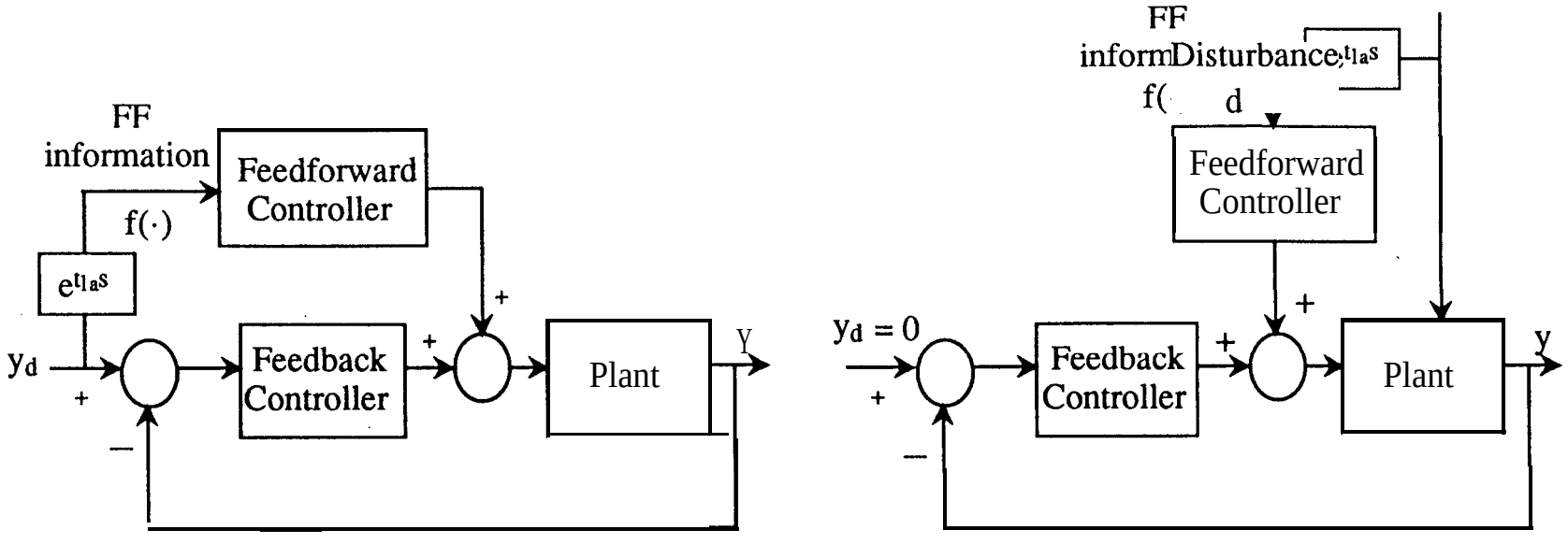

	Feedback Control	Feedback/Feedforward Control	Feedback/Preview Control
FF information used by Feedforward controller (at time t)	None	f(t) Time t	f(t) Time t $t+t_{la}$

f(t) := Yd (t) (tracking problem)
:= d(t) (regulation problem)

t_{la} := preview time

Figure 1 Structure of Feedback, Feedforward, and Preview Control Systems

3. Optimal$_L$ Preview Control for Vehicle Lateral Guidance

It has been shown [1] that in the design of the vehicle lateral controller based on the FSLQ control theory, the frequency-dependent ride quality index can be explicitly included in the cost function. The ride quality is represented by a term which consists of weighted lateral acceleration components in a specified frequency band. There have been several frequency dependent ride quality standards proposed ([22]-[24]). They are useful in the selection of the weighting factor in the performance index. The high-frequency stability robustness of the closed loop system can be improved by properly choosing the weighting matrices on the lateral tracking error terms in the cost function. In [1], the weighting matrices on tracking error terms are shaped so that the controller responds to the changes in road curvature but not to the high frequency components in the error signal due to measurement noise. The FSLQ problem is solved by augmenting the original system, and transforming it into a standard LQ problem [10].

In the following, a FSLQ problem with preview is developed. The resulting algorithm retains all the advantages of the FSLQ control algorithm as described above. Furthermore, the preview action utilizes the future road curvature information so that the transient tracking error and lateral acceleration can be reduced simultaneously. The linearized system equation for the front-wheel-steered vehicle is [1]:

$$\frac{d}{dt}\begin{bmatrix} y_r \\ \dot{y}_r \\ \varepsilon-\varepsilon_d \\ \dot{\varepsilon}-\dot{\varepsilon}_d \end{bmatrix} = \begin{bmatrix} 0 & 1 & 0 & 0 \\ 0 & \frac{A_1}{V} & -A_1 & \frac{A_2}{V} \\ 0 & 0 & 0 & 1 \\ 0 & \frac{A_3}{V} & -A_3 & \frac{A_4}{V} \end{bmatrix} \begin{bmatrix} y_r \\ \dot{y}_r \\ \varepsilon-\varepsilon_d \\ \dot{\varepsilon}-\dot{\varepsilon}_d \end{bmatrix} + \begin{bmatrix} 0 \\ B_1 \\ 0 \\ B_2 \end{bmatrix} \delta + \begin{bmatrix} 0 \\ A_2-V^2 \\ 0 \\ A_4 \end{bmatrix} \frac{1}{\rho} = A\underline{x} + B\delta + Dw \qquad (1)$$

where δ is the front-wheel steering angle, y_r is the lateral deviation of the mass center from the reference, ε is the yaw angle of the vehicle, and ε_d is the desired yaw angle determined by the road curve. ρ is the radius of curvature, and $w = \frac{1}{\rho}$ is the curvature of the road. A_i's and B_i's depend on vehicle parameters, and are defined as follows:

$$\begin{aligned} A_1 &= \frac{-2(C_{sf}+C_{sr})}{m} & A_2 &= \frac{-2\,(C_{sf}\,l_1^2 + C_{sr}\,l_2^2)}{I_z} \\ A_3 &= \frac{2\,(C_{sr}\,l_2 - C_{sf}\,l_1)}{m} & B_1 &= \frac{2}{m}C_{sf} \\ A_4 &= \frac{2\,(C_{sr}\,l_2 - C_{sf}\,l_1)}{I_z} & B_2 &= \frac{2l_1\,C_{sf}}{I_z} \end{aligned} \qquad (2)$$

where m and I_z are the mass and moment of inertia about the vertical axis of the vehicle, respectively, V is the vehicle speed, l_1 and l_2 are the distance from the mass center to the front and rear axle, respectively, and C_{sf} and C_{sr} are the tire cornering stiffness of the front and rear wheels, respectively. The output y_s, taken as the measurement of lateral deviation from a sensor located at a distance d_s ahead of the mass center, can be expressed as:

$$y_s(t) = y_r(t) + d_s\,(\,\varepsilon(t) - \varepsilon_d(t)\,) = [\,1, 0, d_s, 0\,]\,\underline{x}(t) \tag{3}$$

The performance index introduced in [1] is:

$$J = \frac{1}{2\pi}\int_{-\infty}^{\infty}\Big[a^*(j\omega)\frac{q_a^2}{1+\lambda_a^2\omega^2}a(j\omega) + y_r^*(j\omega)\frac{q_y^2}{1+\lambda_y^2\omega^2}y_r(j\omega) \tag{4}$$

$$+(\varepsilon(j\omega)-\varepsilon_d(j\omega))^*\frac{q_\varepsilon^2}{1+\lambda_\varepsilon^2\omega^2}(\varepsilon(j\omega)-\varepsilon_d(j\omega))+y_s^*(j\omega)\frac{q_i^2}{(j\omega)^2}y_s(j\omega)+\delta^*(j\omega)\delta(j\omega)\Big]d\omega$$

where a is the difference between the lateral acceleration $\ddot{y}_a$ and its desired value $\frac{V^2}{\rho}$. The coefficients q_a and λ_a are chosen so that the first term in J represents the ride quality. The coefficients of the next three terms in J are chosen so that the controller reacts to the road curves quickly but is less responsive to the high frequency measurement noises (refer to [1] for details). The FSLQ control problem is solved by defining the following augmented state variables:

$$z_1(s) \equiv \frac{q_a}{1 + \lambda_a s}a(s) \tag{5}$$

$$z_2(s) \equiv \frac{q_y}{1 + \lambda_y s}y_r(s) \tag{6}$$

$$z_3(s) \equiv \frac{q_\varepsilon}{1 + \lambda_\varepsilon s}(\varepsilon(s) - \varepsilon_d(s)) \tag{7}$$

$$z_4(s) \equiv \frac{q_i}{s}y_s(s) \tag{8}$$

The FSLQ problem is now transformed into a standard LQ problem with the following dynamic equation and performance index:

$$\dot{\underline{x}}_e(t) = A_e\underline{x}_e(t) + B_e\delta(t) + D_e\,w(t) \tag{9}$$

$$J = \lim_{t_f\to\infty}\frac{1}{2}\int_0^{t_f}[\underline{x}_e^T(t)Q\underline{x}_e(t) + \delta^T(t)R\delta(t)]\,dt \tag{10}$$

where $\underline{x}_e = [\underline{x}^T, z_1, z_2, z_3, z_4]^T$ is the augmented eighth order state vector, A_e, B_e, D_e are the augmented system matrices, and the weighting matrices Q and R are:

$$Q = \begin{vmatrix} \mathbf{0} & \mathbf{0} & \mathbf{0} & \mathbf{0} & \mathbf{0} & \mathbf{0} & \mathbf{0} & \mathbf{0} \\ \mathbf{0} & \mathbf{0} & \mathbf{0} & \mathbf{0} & \mathbf{0} & \mathbf{0} & \mathbf{0} & \mathbf{0} \\ \mathbf{0} & \mathbf{0} & \mathbf{0} & \mathbf{0} & \mathbf{0} & \mathbf{0} & \mathbf{0} & \mathbf{0} \\ \mathbf{0} & \mathbf{0} & \mathbf{0} & \mathbf{0} & \mathbf{0} & \mathbf{0} & \mathbf{0} & \mathbf{0} \\ 0 & 0 & 0 & 0 & 1 & 0 & 0 & 0 \\ 0 & 0 & 0 & 0 & 0 & 1 & 0 & 0 \\ 0 & 0 & 0 & 0 & 0 & 0 & 1 & 0 \\ 0 & 0 & 0 & 0 & 0 & 0 & 0 & 1 \end{vmatrix} \quad R = 1 \tag{11}$$

where the weighting coefficients q_a, q_y, q_ε, and q_i are absorbed in the augmented state variables, z_i's. It can be shown that the performance index given by Eq.(4) is equivalent to the one in Eq.(10) following the Parseval's Theorem. In the present preview FSLQ problem, it is assumed that the disturbance $w(t)$ within a preview time of t_{la} is available ahead of time: i.e. $\{w(t+\sigma)\ \mathrm{I}\ 0 \le \sigma \le t_{la}\}$ is known at time t.

In the following two sections, the optimal preview control laws are developed for two different scenarios. In section 3.1, the road curvature w is assumed to be available as preview information. In section 3.2, future information on both the road curvature w and the superelevation angle γ is assumed to be available.

3.1 Preview Control for Road Curvature

Like other linear quadratic optimal control problems, the optimal preview control problem is solved by Dynamic Programming [25]. The performance index to be minimized is defined by:

$$J(t) = \frac{1}{2}\int_t^{t_f} [\underline{x}_e^T(\tau) Q \underline{x}_e(\tau) + \delta^T(\tau) R \delta(\tau)]\, d\tau \tag{12}$$

where Q and R are as defined in Eq.(11). The following equation can be derived from the principle of optimality:

$$0 = \min_{\delta(t)} \left\{ \frac{1}{2}\underline{x}_e^T(t) Q \underline{x}_e(t) + \frac{1}{2}\delta^T(t) R \delta(t) + \frac{dJ^*(t)}{dt} \right\} \tag{13}$$

where $J^*(t)$ is the optimal cost function among all $J(t)$ defined in Eq.(12), and $\frac{d}{dt}$ denotes the total differentiation with respect to time. The Hamiltonian H is defined as:

$$H \equiv \frac{1}{2}\underline{x}_e^T Q \underline{x}_e + \frac{1}{2}\delta^T R \delta + \frac{\partial J^*}{\partial \underline{x}_e}(A_e \underline{x}_e + B_e \delta + D_e w) \tag{14}$$

The optimal control $\delta_{opt}(t)$ can then be obtained from:

$$\frac{\partial H}{\partial \delta}\Big|_{\delta=\delta_{opt}} = 0 \tag{15}$$

The minimization of the performance index Eq. (10) requires that the disturbance be specified over the problem duration. However, the preview assumption implies that

only $\{w(t+\sigma) \mid 0 \le \sigma \le t_{la}\}$ isknownattimet. A natural way to specify the disturbance beyond the preview segment is to introduce a disturbance generator described by:

$$\frac{dw(\tau)}{d\tau} = A_w w(\tau) \qquad \tau \ge t + t_{la} \tag{16}$$

where $A_w \le 0$ governs the decay rate of w(z). The optimal preview control algorithm is solved by assuming that the optimal cost function can be expressed by the generalized quadratic form with respect to:

1. the current state vector $\underline{x}_e(t)$
2. disturbance $w(t+\tau)$ in the preview segment $\tau \in [0, t_{la}]$

The optimal cost function is then expressed as:

$$J^*(\underline{x}_e(t), w(t,[0,t_{la}])) \tag{17}$$
$$= \frac{1}{2}\underline{x}_e^T(t)K(t)\underline{x}_e(t) + \frac{1}{2}\int_0^{t_{la}}\int_0^{t_{la}} w^T(t,l_1)K_w(t,l_1,l_2)w(t,l_2)dl_1dl_2$$
$$+ \frac{1}{2}w^T(t+t_{la})K_d(t)w(t+t_{la}) + \underline{x}_e^T(t)\int_0^{t_{la}} F_1(t,l)w(t,l)dl + \underline{x}_e^T(t)F_2(t)w(t+t_{la})$$

where $w(t, l) \equiv w(t + l)$. The optimal control law can then be derived from Eq.(13)-(17):

$$\delta_{opt}(t) = -R^{-1}B_e^T[K(t)\underline{x}_e(t) + \int_0^{t_{la}} F_1(t,l)w(t,l)dl + F_2(t)w(t+t_{la})] \tag{18}$$

The details of deriving Eq.(18) is given in Appendix. Rearranging Eq. (A.7), we obtain the following equations:

$$A_e^TK(t) - K(t)B_eR^{-1}B_e^TK(t) + \dot{K}(t) + K(t)A_e + Q = 0 \tag{19}$$
$$K(t_f) = 0$$

$$\frac{\partial F_1^T(t,l)}{\partial t} = \frac{\partial F_1^T(t,l)}{\partial l} + F_1^T(t,l)[B_eR^{-1}B_e^TK(t) - A_w] \tag{20}$$
$$F_1^T(t,0) = D_e^TK(t)$$

$$\dot{F}_2^T(t) = F_2^T(t)B_eR^{-1}B_e^TK(t) - F_1^T(t,t_{la}) - F_2^T(t)A_e - A_w^TF_2^T(t) \tag{21}$$
$$F_2(t_f) = 0$$

$$\dot{K}_d(t) = F_2^T(t)B_eR^{-1}B_e^TF_2(t) - A_w^TK_d(t) \tag{22}$$
$$K_d(t_f) = 0$$

$$\frac{\partial K_w(t,l_1,l_2)}{\partial t} = \frac{\partial K_w(t,l_1,l_2)}{\partial l_1} + \frac{\partial K_w(t,l_1,l_2)}{\partial l_2} + F_1^T(t,l_1)B_e R^{-1}B_e^T F_1(t,l_2) \qquad (23)$$

$$K_w(t, t_{la}, l) = F_2^T(t)B_e R^{-1}B_e^T F_1(t, l)$$

$$K_w(t, 0, l) = D_e^T F_1(t, l)$$

where the boundary conditions of Eq.(19), (21) and (22) are obtained from general preview control design procedures (refer to [20] for details). It can be seen from Eq.(18) that the optimal control signal depends on $K(t)$, $w(t,l)$, $F_1(t,l)$ $(0 \le l \le t_{la})$ and $F_2(t)$ only; therefore, Eqs.(22) and (23) are not solved in this report. However, we would like to point out that both (22) and (23) have proper boundary values and thus can be solved after solving Eq.(19)-(21). Furthermore, since we are deriving the FSLQ-preview control law, the problem duration is infinite. Therefore, the steady state solutions of Eqs. (19)-(21) are used, and the boundary conditions in Eq.(19)-(21) do not affect the control law.

It can be seen from Eq.(18) that the preview control law consists of three terms, one feedback term and two feedforward terms. The first term is exactly the same as the feedback control signal in the FSLQ control algorithm without the preview assumption (compare (19) with results in [1]). The second term is the preview action to deal with the disturbance signal (road curvature) within the preview segment. The third term is the preview action to cope with the disturbance beyond the preview segment.

3.2 Preview Control for Road Superelevation

In this section, the road superelevation angle (besides the road curvature) is considered. It is modeled in the system dynamic equation, and its value in the preview segment is assumed to be available. Road superelevation affects not only the lateral tracking performance but also the estimation of the cornering stiffness. If the information on the road superelevation is not available to the controller, a large transient tracking error may occur.

The vehicle lateral dynamic equation, which includes the road superelevation angle y is

$$\ddot{y}_r = \frac{A_1}{V}\dot{y}_r - A_1(\varepsilon - \varepsilon_d) + \frac{A_2}{V}(\dot{\varepsilon} - \dot{\varepsilon}_d) + B_1\delta + \frac{A_2 - V^2}{\rho} - g\gamma \qquad (24)$$

It is assumed that the road superelevation angle y is the same at the front and rear axles of the vehicle. Therefore, the dynamic equation which governs the yaw motion is not changed. Since y is assumed to be small, siny $\simeq$ y. There are two approaches to developing the optimal preview control law which handles both the road curvature w and superelevation angle γ:

1. In the first approach, the system dynamic equations are written as:

$$\dot{x}_e(t) = A_e x_e(t) + B_e \delta(t) + [\, D_{e1} D_{e2} \begin{bmatrix} w(t) \\ \gamma(t) \end{bmatrix} \tag{25}$$

The optimal preview control law can then be obtained by following the procedures described in section 3.1. However, because two disturbances enter the system, the size of the feedforward gain matrices $F_1(l)$ and F_2 will be doubled.

2. We may incorporate the road curvature information (p) and the superelevation information (γ) to form an effective radius of curvature (p'). The preview controller developed in section 3.1 can then be used to offset the effects due to both the road curvature and the superelevation by substituting p with p'. It can be seen that the only difference between the "superelevated" and "non-superelevated" dynamic equations is the extra term $-g\gamma$ in (24). If we define an "effective radius of curvature" (p') by:

$$\rho' = \frac{A_2 - V^2}{A, -V^2 - \rho g \gamma} \times \rho \tag{26}$$

the effects of both road radius and superelevation angle are included in ρ'. Note that in Eq.(26) g represents the gravitational constant. Figure 2 shows the relationship between γ and p'. When γ has the same sign as p', the curve becomes sharper for the vehicle due to the road superelevation.

It will be shown in section 5 by simulations that the effective radius of curvature p' accurately represents the combination of the road superelevation and radius information, for the purposes of both feedforward control and tire cornering stiffness estimations. Therefore, the second approach is used in this report.

4. Frequency Domain Analysis

By using the steady state gains of K, F_1 and F_2, the effect of the preview control can be interpreted from the viewpoint of frequency domain. The steady state solution (K_{ss}) of Eq.(19) is obtained from the Algebraic Riccati Equation (ARE), and the steady-state solutions of F_1 and F_2 are

$$F_1(l) = e^{A_c^T l} K_{ss} D_e \qquad 0 \le 1 \le t_{la} \tag{27}$$

$$F_2 = -(A_c^T + A_w I)^{-1} e^{A_c^T t_{la}} K_{ss} D_e \tag{28}$$

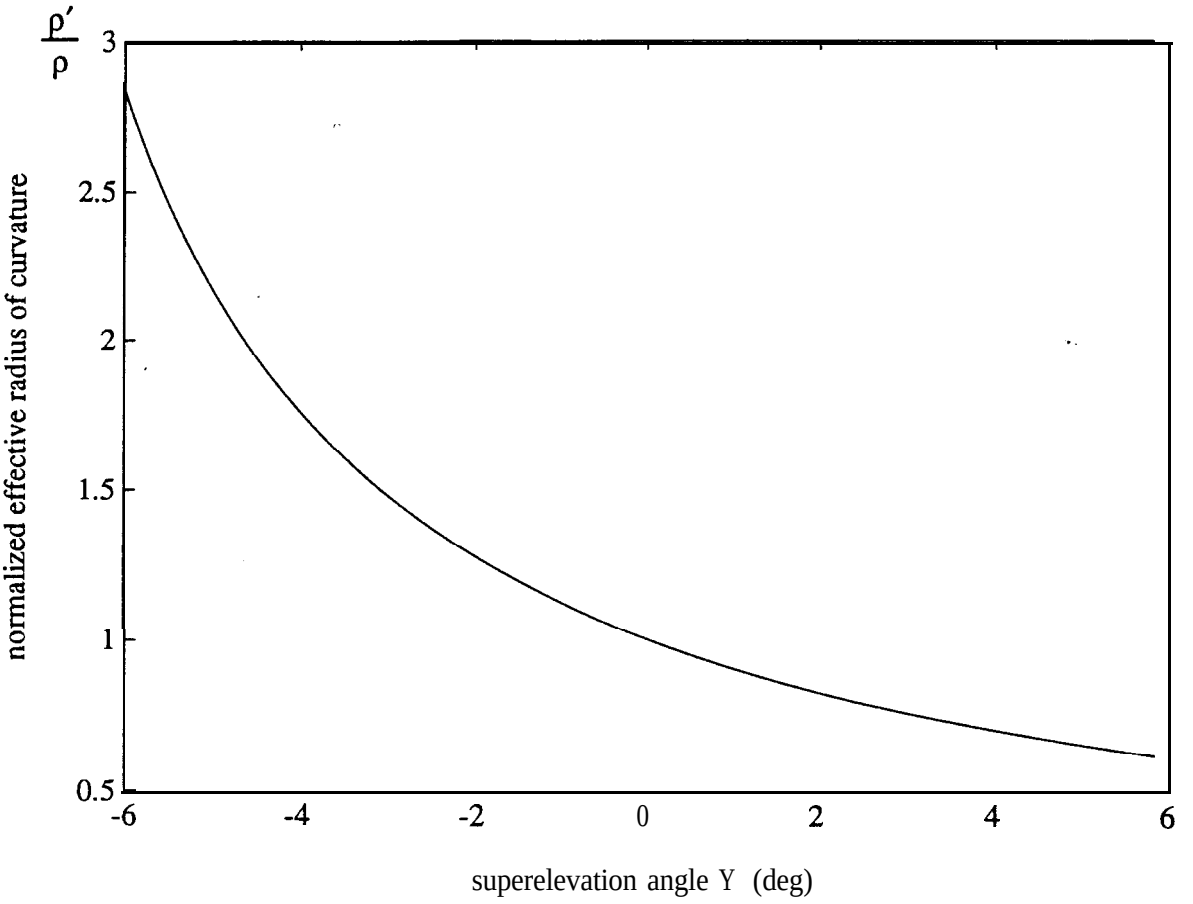

Figure 2 Normalized radius of curvature

respectively, where $\mathbf{A}, \equiv A, - B_e R^{-1} B_e^T K_{ss}$ is the closed loop system matrix. It should be noted that Eq.(28) is no longer true if there is more than one disturbance signal in the system.

Substituting (27) and (28) into (18), we obtain:

$$\delta_{opt}(s) = -R^{-1}B_e^T[K_{ss}\underline{x}_e(s) + \int_0^{t_{la}} F_1(l)e^{ls}dl\ w(s) + F_2 e^{t_{la}s}w(s)] \qquad (29)$$
$$= -R^{-1}B_e^T[K_{ss}\underline{x}_e(s) + \int_0^{t_{la}} e^{A_c^T l}K_{ss}D_e e^{ls}dl\ w(s) - (A_c^T + A_w I)^{-1}e^{A_c^T t_{la}}K_{ss}D_e e^{t_{la}s}w(s)]$$

To simplify Eq.(29), we note the following relation:

$$\int_0^{t_{la}} e^{A_c^T l}e^{ls}dl = \frac{1}{s}e^{A_c^T l}e^{ls}\Big|_0^{t_{la}} - \int_0^{t_{la}}\frac{1}{s}A_c^T e^{A_c^T l}e^{ls}dl = \frac{1}{s}(e^{A_c^T t_{la}}e^{t_{la}s} - I) - \frac{1}{s}A_c^T\int_0^{t_{la}} e^{A_c^T l}e^{ls}dl \qquad (30)$$

or

$$\int_0^{t_{la}} e^{A_c^T l}e^{ls}dl = (sI + A_c^T)^{-1}(e^{A_c^T t_{la}}e^{t_{la}s} - I) \qquad (31)$$

Substituting (31) into (29), we obtain:

$$\delta_{opt}(s) = -R^{-1}B_e^T K_{ss}\underline{x}_e(s) - R^{-1}B_e^T(sI + A_c^T)^{-1}(e^{A_c^T t_{la}}e^{t_{la}s} - I)K_{ss}D_e w(s) \qquad (32)$$
$$+ R^{-1}B_e^T(A_c^T + A_w I)^{-1}e^{A_c^T t_{la}}K_{ss}D_e e^{t_{la}s}w(s)$$

From Eq. (32) and (9), we obtain the transfer function from road curvature w to output y_s:

$$G_{y_s w}(s) = c_e(sI - A_c)^{-1}[D_e - B_e R^{-1}B_e^T(sI + A_c^T)^{-1}(e^{A_c^T t_{la}}e^{t_{la}s} - I)K_{ss}D_e \qquad (33)$$
$$+ B_e R^{-1}B_e^T(A_c^T + A_w I)^{-1}e^{A_c^T t_{la}}K_{ss}\underline{D}_e e^{t_{la}s}]$$

where c_e = [1,0,d_s,0,0,0,0,0] is the augmented output matrix and is obtained noting Eq.(3).

To investigate the effect of preview control on ride quality, the transfer function from w to lateral acceleration $\ddot{y}_a$ is also derived. Note that the total lateral acceleration can be computed from:

$$\ddot{y}_a \approx \ddot{y}_r + \frac{V^2}{\rho} = c_{acc}\underline{x}_e + B_1\delta + D_1 w + \frac{V^2}{\rho} = C_{acc}\underline{x}_e + B_1\delta + D_1 w + V^2 w \qquad (34)$$

where $c_{acc} = [0, \frac{A_1}{V}, -A_1, \frac{A_2}{V}, O, O, O, O]$ is the lateral acceleration output matrix. Substituting (32) into (34), the following transfer function is obtained:

$$G_{\ddot{y}_a w}(s) = (c_{acc} - B_1 R^{-1} B_e^T K_{ss})(sI - A_c)^{-1}[D_e - B_e R^{-1} B_e^T (sI + A_c^T)^{-1}(e^{A_c^T t_{la}} e^{t_{la} s} - I) K_{ss} D_e \quad (35)$$
$$+ B_e R^{-1} B_e^T (A_c^T + A_w I)^{-1} e^{A_c^T t_{la}} K_{ss} D_e e^{t_{la} s}] + B_1[-R^{-1} B_e^T (sI + A_c^T)^{-1}(e^{A_c^T t_{la}} e^{t_{la} s} - I) K_{ss} D_e$$
$$+ R^{-1} B_e^T (A_c^T + A_w I)^{-1} e^{A_c^T t_{la}} K_{ss} D_e e^{t_{la} s}] + A_2$$

The transfer functions $G_{y_s w}(s)$ and $G_{\ddot{y}_a w}(s)$ are plotted in Figure 3 and 4 respectively, for the nominal system parameters in Table 1. It can be seen that the preview control signal improves both the tracking error in the low-frequency region and the lateral acceleration in the high frequency region. The following points should be noted:

(1) The preview controller improves the low-frequency tracking performance up to a certain frequency, beyond which (when the road curvature changes more quickly) there is no improvement at all. This frequency was found to be the closed loop cut-off frequency of the transfer function $G_{y_s \delta}$ (see Figure 5).

(2) Preview control steering action reduces the high-frequency lateral acceleration component. At low frequency, lateral acceleration is governed by the relation $\ddot{y}_a = \frac{V^2}{\rho}$, and cannot be reduced by preview actions. Therefore, the magnitude of $G_{\ddot{y}_a w}(j\omega)$ approaches V^2 as $\omega \rightarrow 0$ for both the previewed and unpreviewed cases.

5. Simulation Results

It has been pointed out that the preview time should be about three times as large as the inverse of the closed loop bandwidth[12,14], which is about 0.17 seconds in the present problem. Therefore, the preview time of 0.5 second is used. Beyond this value, the increase in t_{la} only results in negligible improvement in the performance index. A_w in the disturbance dynamics (16) is chosen to be zero. That is, the road curvature is assumed to be unchanged beyond the preview segment $[t, t+t_{la}]$. Furthermore, to implement the preview control law in real-time, a summation is used to approximate the integration term in (18).

The hypothetical test track used in the simulations consists of a curved section connecting two straight sections. The parameters utilized in the simulations are the nominal values listed in Table 1, unless otherwise stated. A first order time-lag model with a 33 *msec* time constant is used to describe the steering actuator dynamics. The sampling time for measurement is assumed to be 10 msec. The lateral tracking error is assumed to be obtained intermittently from discrete markers on the road center. The discrete markers are assumed to be placed at 0.9m spacing, which determines not only the measurement rate of the tracking error, but also the updating rate of the preview

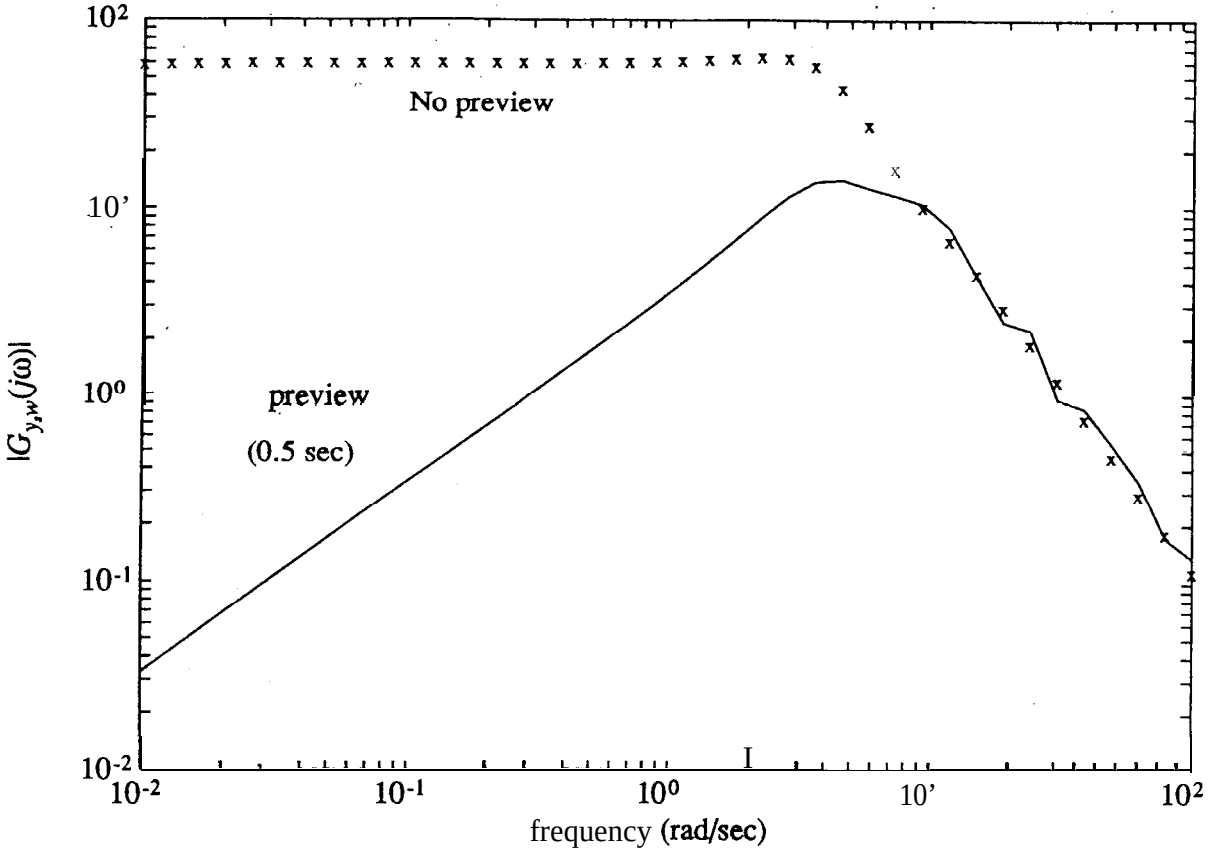

Figure 3 Frequency response of $G_{y,w}(s)$

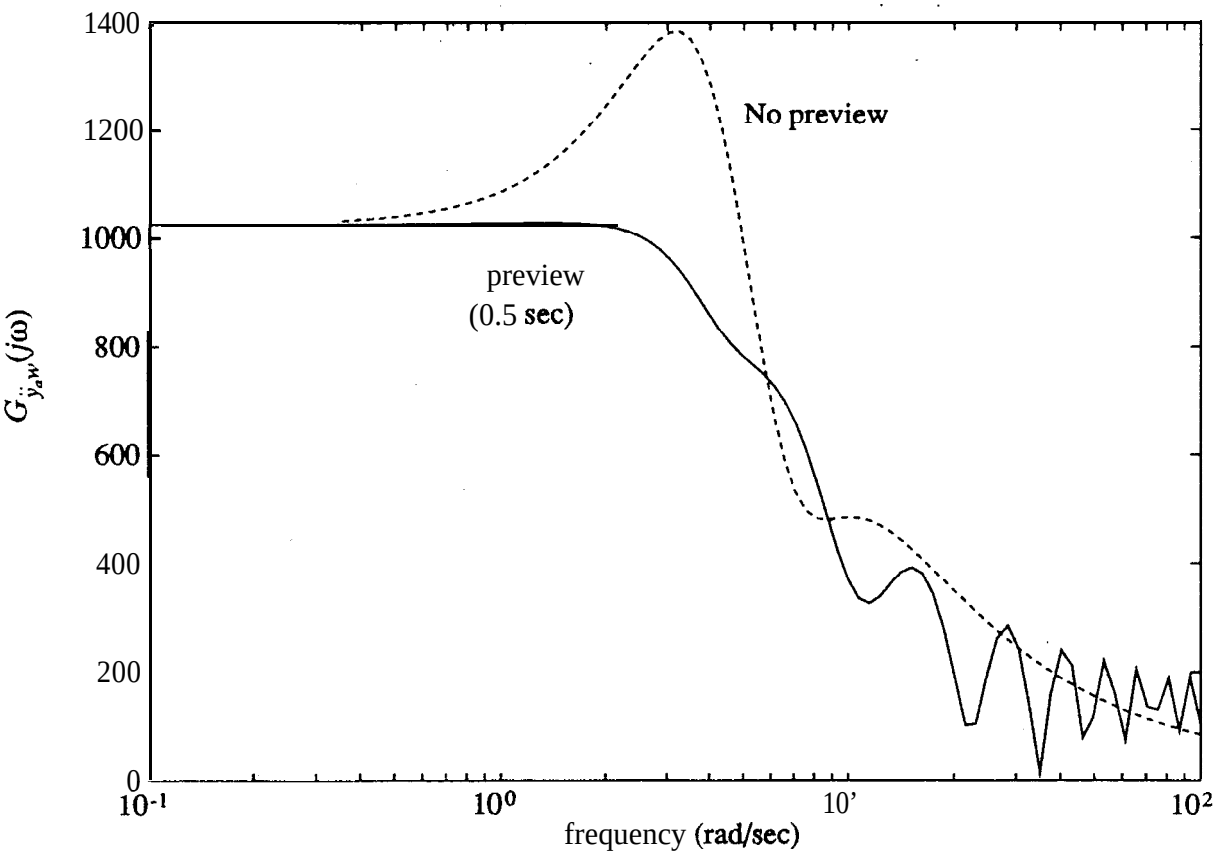

Figure 4 Frequency response of $G_{\ddot{y}_a w}(s)$

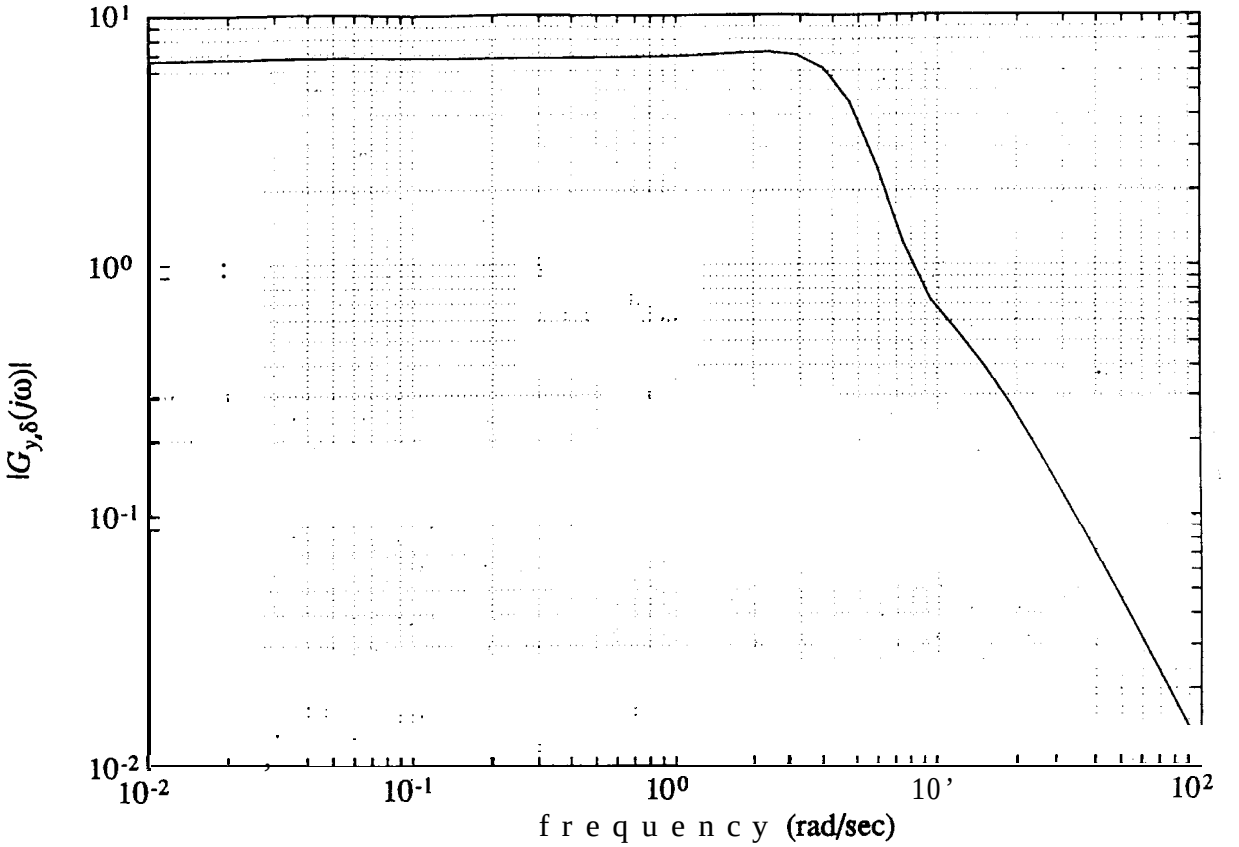

Figure 5 Frequency response of $G_{y,\delta}(s)$

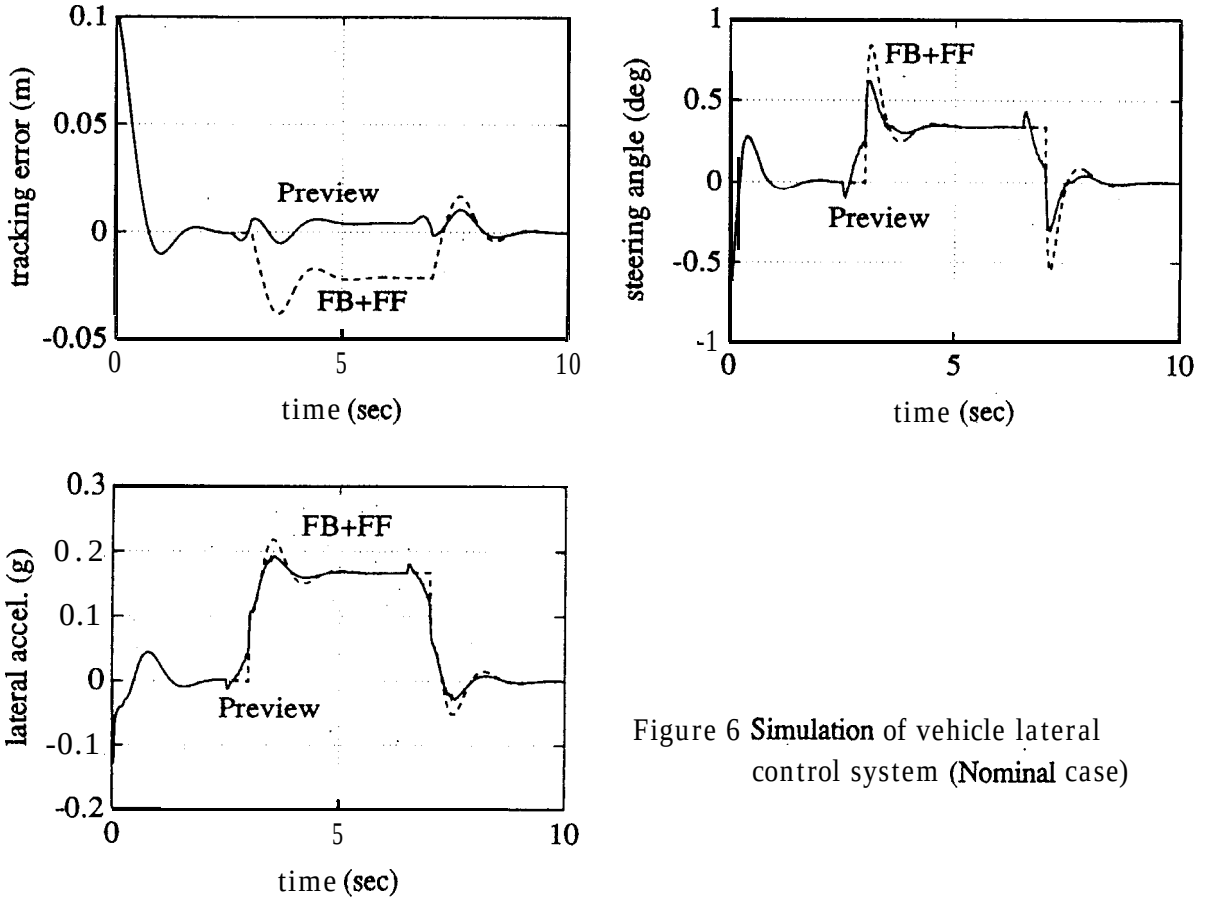

Figure 6 Simulation of vehicle lateral control system (Nominal case)

(curvature and superelevation) information. The average tire cornering stiffness (C,) is estimated based on the vehicle dynamic equations for gain scheduling purposes (see [1] for details).

Nominal Case

Figure 6 shows the simulation results when the vehicle is steered by the preview control law. The responses of the vehicle controlled by the FSLQ feedback plus steady-state feedforward control law (see [1] for details) are also presented for comparison. The feedforward control law sends out the corresponding steering angle for current road curvature. It can be seen that the preview control law improves the tracking performance significantly and at the same time reduces the peak value of the lateral acceleration.

Variable V and C_s

The responses of the vehicle under different speeds V are plotted in Figure 7. The tracking error when the vehicle speed is 10 *mlsec* is much larger than that at a higher speed, This is attributed to the fact that the control law design is based on the linear model, and the difference between the linear model and the nonlinear model (which is used for all the simulations) increases as steering angle increases. Figure 8 shows the responses of the vehicle driving at the nominal speed, while a 30-meter-long patch of ice (which reduces C_{sf} and C_{sr} to their minimum values) is present in the middle of the curve. The tracking error is always smaller than the designated measurement range (20 cm) of the discrete magnetic marker system [15]. Figure 9 shows the simulation results when the gain of the controller is fixed (for the nominal system) while all other conditions remain the same as the simulation run in Figure 8. It can be seen that the fixed gain controller does not respond to the change in the road surface condition, and results in a much higher peak value of the tracking error (30 cm).

Road Sunerelevation

Figure 10 shows the results of the vehicle driving on a straight but super-elevated road. Two sets of results are presented. In the first run, the effective radius of curvature p' is used (which includes the superelevation (SE) information). In the second run, the original road radius of curvature is used. It can be seen that a large error occurs in the estimation of C_s in the second run, and the tracking performance deteriorates noticeably.

Variable t_{la}

It can be seen from Figure 11 that when the preview time t_{la} is long (1 second), reverse action appears when the vehicle enters or leaves the curve. In other words, the vehicle is steered to the opposite direction from the curve, and then back to the right direction. The reverse action disappears as the preview time is decreased ($\leq$ 0.3 second). It can be seen from Eq. (18) that the reverse action is determined by the term $-R^{-1}B_e^TF_2$. Reverse action appears when $-R^{-1}B_e^TF_2$ is negative. Figure 12 shows the

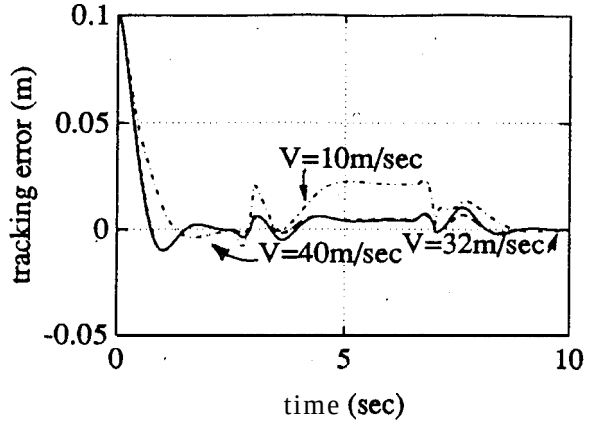

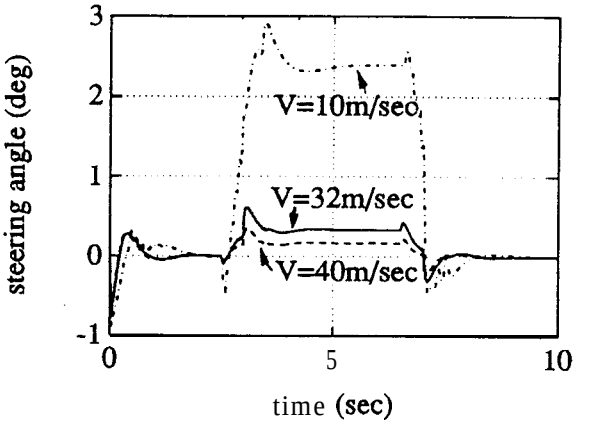

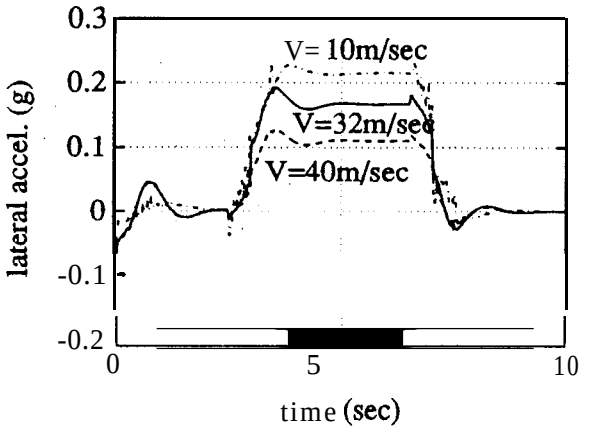

Figure 7 Simulation of vehicle lateral control system (Variable V)

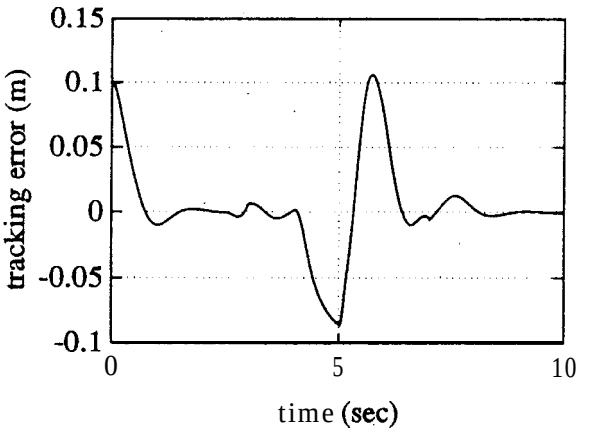

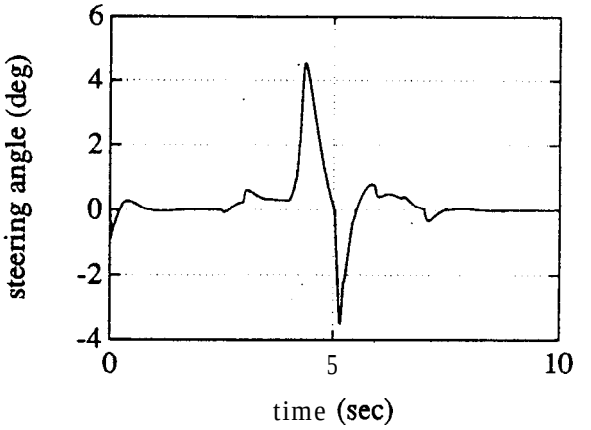

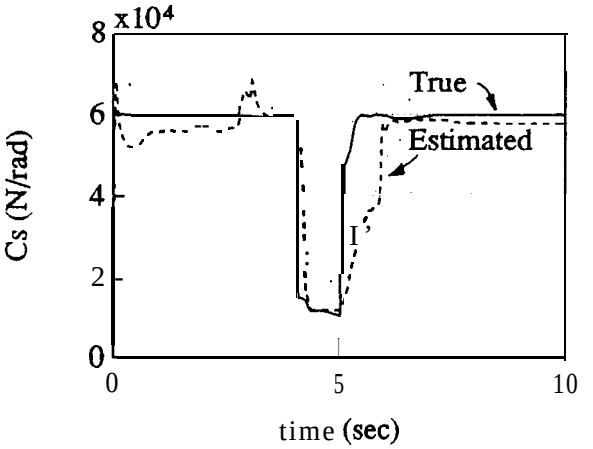

Figure 8 Simulation of vehicle lateral control system (Variable Cs)

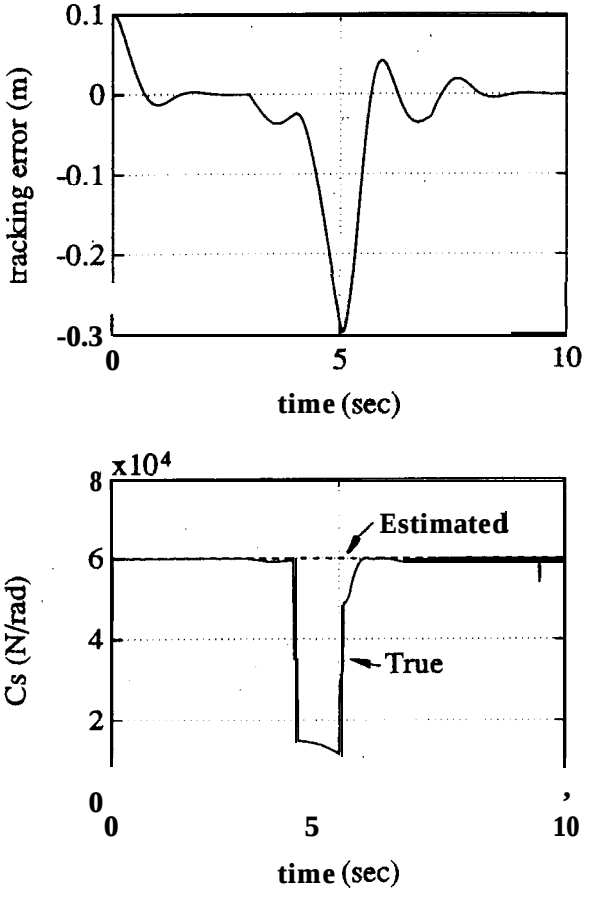

Figure 9 Simulation of vehicle lateral control system (Var. Cs-fixed gain)

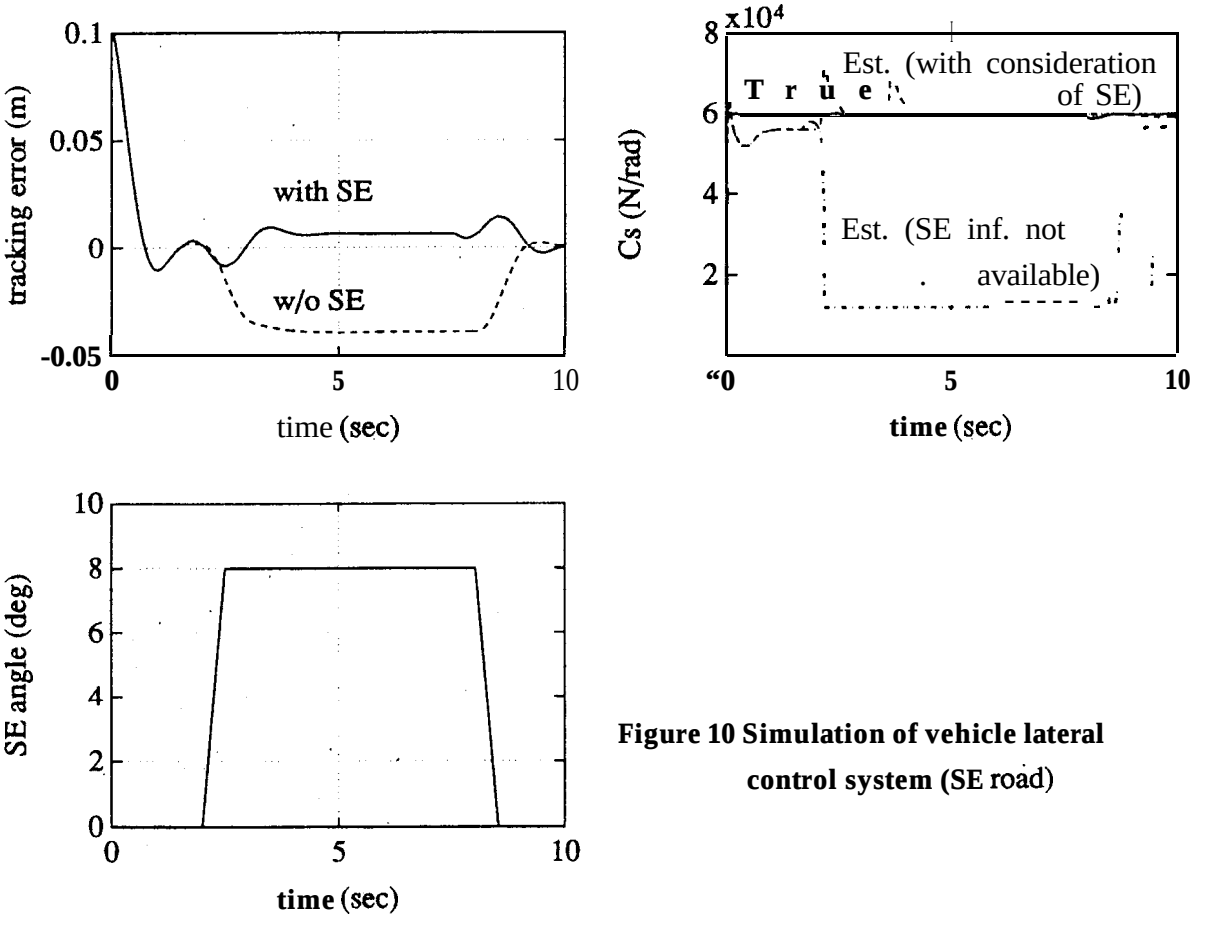

Figure 10 Simulation of vehicle lateral control system (SE road)

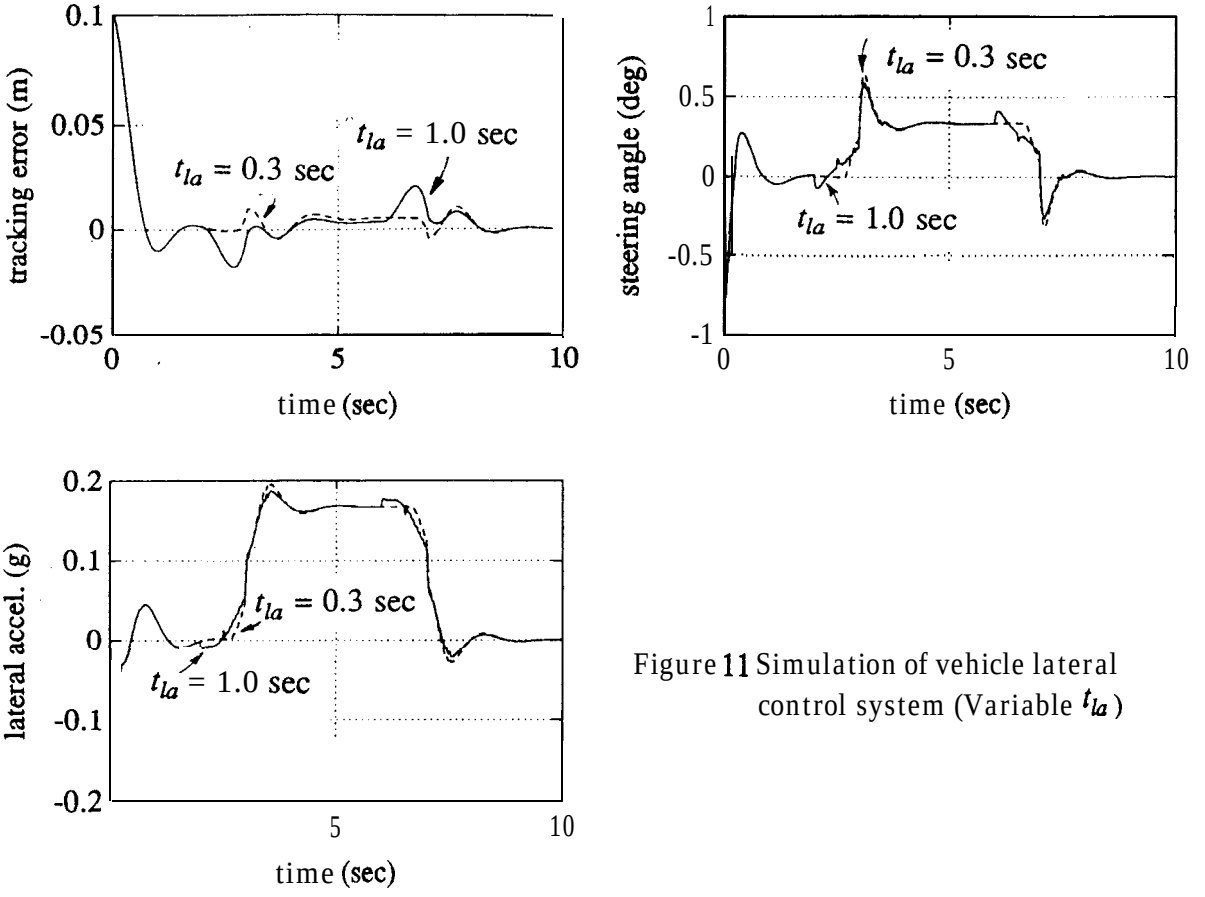

Figure 11 Simulation of vehicle lateral control system (Variable t_{la})

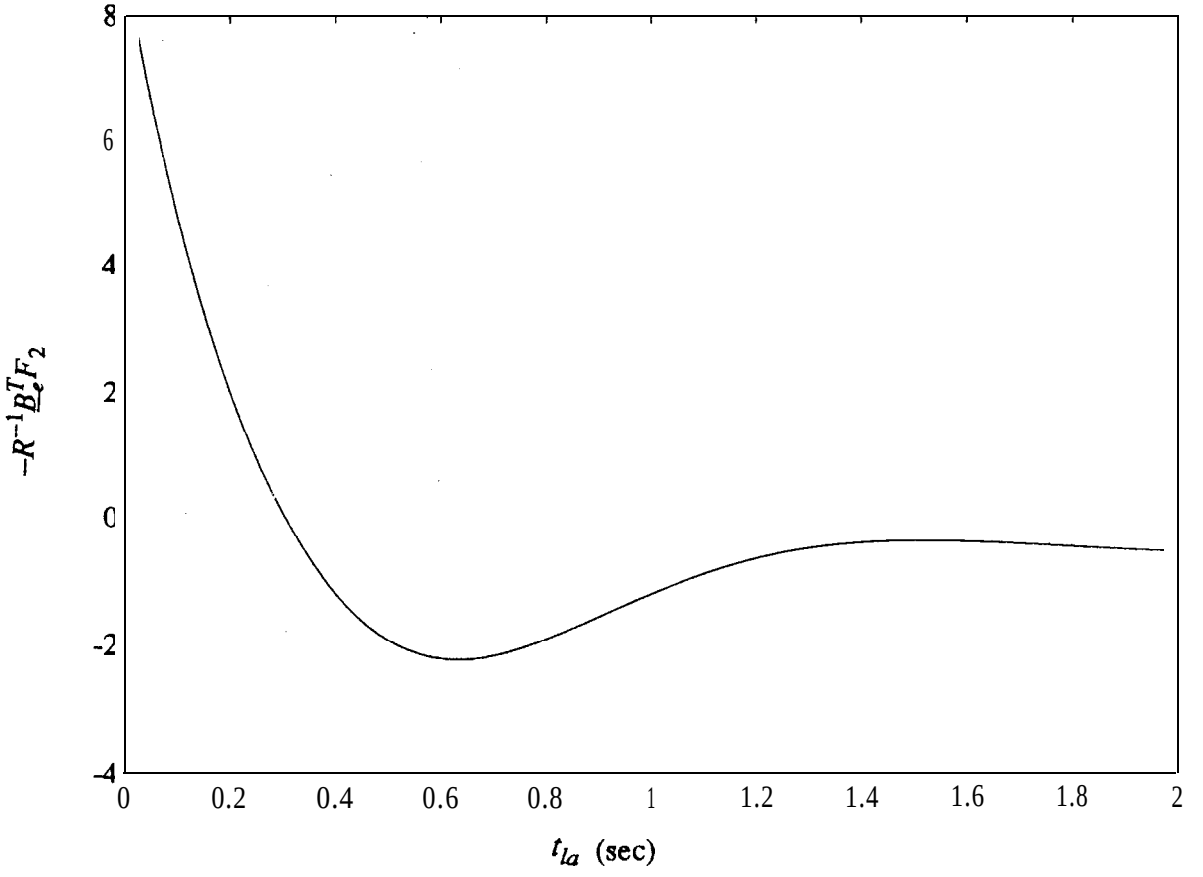

Figure 12 Value of $-R^{-1}\underline{B}_e^T F_2$ as function of t_{la}

value of $-R^{-1}B_e^T F_2$ as t_{la} varies. It can be seen that reverse action occurs whenever t_{la} is greater than 0.3 seconds; and reaches its peak value at around t_{la} = 0.65 seconds.

6. Conclusions

The preview control action, which utilizes the curvature and superelevation of the road ahead, has been incorporated in the vehicle lateral control law. The controller design was based on the FSLQ optimal control theory. Results of the frequency-domain analysis show that the preview control law simultaneously improves the low frequency tracking performance and reduces high frequency lateral acceleration. Furthermore, results from the numerical simulation study show that the preview control algorithm enables the vehicle to track the center of a lane with a small tracking error (< 20 cm) under all the hypothetical scenarios.

7. References

1. Peng, H., Tomizuka, M., "Lateral Control of Front-Wheel-Steering Rubber-Tire Vehicles," Publication of PATH project, ITS, UC Berkeley, UCB-ITS-PRR-90-5, July 1990.

2. Gupta, N., "Frequency-Shaped Cost Functionals: Extension of Linear-Quadratic-Gaussian Design Methods," Journal of Guidance and Control, Vo1.3, No.6, pp. *529-535,* Nov-Dee 1980.

3. Anderson, B.D.O., Moore, J.B., ***Optimal Control -- Linear Quadratic Methods,*** Chapter 9, Prentice Hall, 1990.

4. Roland, R. D., Sheridan, T. B., "Simulation Study of the Driver's Control of Sudden Changes in Previewed Path", MIT, Dept. of Mech. Eng., Report DSR 74920-1, 1967.

5. McRuer, D. T., Allen, R. W., Weir, D. H., Klein, R. H., "New Results in Driver Steering Control Models," Human Factors, Vo1.19, No.4, 1977.

6. McLean, J. R., Hoffmann, E. R., "Analysis of Drivers' Control Movements", Human Factors, 13(5), 407-418, 1971.

7. McRuer, D., Weir, D. H. "Theory of Manual Vehicular Control", Ergonomics, Vol. 12, No. 4, 599-633, 1969.

8. McLean, J. R., Hoffmann, E. R., "The Effects of Restricted Preview on Driver Steering Control and Performance", Human Factors, 15(4), 421-430, 1973.

9. Godthelp, H., "Vehicle Control During Curve Driving," Human Factors, Vo1.28, No.2, 1986.

10. Kondo, M., Ajimine, A., "Drivers' sight point and Dynamics of the Driver-Vehicle-System Related to it," SAE Technical paper, 680104, 1968.

11. Liu, S. M., Frank, A. A., "The Use of a Forward Looking Sensor for the Lateral Control of Highway Vehicles," Report not formally published.

12. Lee, A. Y., "A Preview Steering Autopilot Control Algorithm for Four-Wheel-Steering Passenger Vehicles," Advanced Automotive Technologies, pp. 83-98, ASME, 1989.

13. Tomizuka, M., Rosenthal, D. E., "On the Optimal Digital State Vector Feedback Controller With Integral and Preview Actions," Transactions of the ASME, Vol. 101, pp.172-178, June, 1979.

14. Tomizuka, M., Whitney, D., E., "Optimal Discrete Finite Preview Problems (Why and How is Future Information Important?)', Trans. of ASME, J. of Dynamic Systems, Measurement, and Control, pp.319-325, Dec. 1975.

15. Zhang, W., Parsons, R., West, T., "An Intelligent Roadway Reference System for Vehicle Lateral Guidance/Control," Proc. ACC, San Diego, 1990.

16. Oldenberger, R., Chang, R.C.C., "Optimal Nonlinear Control for Step and Pulse Disturbances," Trans. of ASME, J. of Basic Eng., Vo1.87, No.1, March 1965.

17. Sheridan, T.B., "Three Models of Preview Control," IEEE Trans. on Human Factors in Electronics, Vol.HFE-7, No.2, June 1966.

18. Bender, E. K., "Optirnum Linear Preview Control with Application to Vehicle Suspension", Trans. of ASME, J. of Basic Engineering, pp.213-221, Jun. 1968.

19. Tomizuka, M., "Optimum Linear Preview Control with Application to Vehicle Suspension -- Revisited", Trans. of ASME, J. of Dynamic Systems, Measurement, and Control, Vo1.98, No.3, pp.309-315, Sep. 1976.

20. Tomizuka, M., "The Optimal Finite Preview Problem and its Application to Man-Machine Systems," Ph.D. dissertation, M.I.T., Feb. 1974.

21. Tomizuka, M., "The Continuous Optimal Finite Preview Control Problem," Trans. of the Society of Instrument and Control Engineers, Vo1.12, No.1, pp. 7-12 (in Japanese), Feb. 1976.

22. Anonymous, "A Guide to the Evaluation of Human Exposure to Whole Body Vibration," ISO/DIS 263 1, International Organization for Standardization, New York, 1972.

23. Anonymous, "Design Specifications for Urban Tracked Air Cushion Vehicles," U.S. Department of Transportation, Washington D.C., 1972.

24. Janeway, R.N., "Vehicle Vibration Limits to Fit the Passenger," S.A.E. Journal, Vol.56, pp.48-49, Aug. 1948.

25. Bellman, R. E., *Dynamic Programming,* Princeton, Princeton University Press, 1957.

Table 1 Simulation parameters

symbol	meaning	nom. value	min	max
m (kg)	mass	1573	0.85(*)	1.15(*)
I_z (kg–m^2)	mom. of iner.(z)	2783	0.85(*)	1.15(*)
C_{sf} (N/rad)	front cor. stiff.	66000	0.2(*)	1.0(*)
C_{sr} (N/rad)	rear cor. stiff.	53850	0.2(*)	1.0(*)
V (m/sec)	vehicle speed	32	10	40
ρ (m)	radius of curve	630	50	1500
l_1 l_2 (m)	dist. c.g. to axles	1.034 1.491	-	-
d_s (m)	dist. c.g. to magnetometer	1.4	-	-
T_s (sec)	sampling time	0.01	-	-
D_m (m)	marker spacing	0.9	-	-
t_{la} (sec)	preview time	0.5	-	-
$A_{...}$	dist. decay rate	0		

(*) relative to the nominal value

Appendix

To solve the optimal preview control problem, the minimum value of the cost function (12) is expressed by the following generalized quadratic form:

$$
\begin{aligned}
&J^*(\underline{x}_e(t), w(t,[0,l_{la}])) \\
&= \frac{1}{2}\underline{x}_e^T(t)K(t)\underline{x}_e(t) + \frac{1}{2}\int_0^{t_{la}}\int_0^{t_{la}} w^T(t,l_1)K_w(t,l_1,l_2)w(t,l_2)dl_1dl_2 \\
&+ \frac{1}{2}w^T(t+t_{la})K_d(t)w(t+t_{la}) + \underline{x}_e^T(t)\int_0^{t_{la}} F_1(t,\, l)w(t,\, l)dl + \underline{x}_e^T(t)F_2(t)w(t+t_{la})
\end{aligned}
\tag{A.1}
$$

The total differentiation of J^* with respect to time is:

$$
\begin{aligned}
\frac{dJ^*}{dt} &= \frac{1}{2}[\dot{\underline{x}}_e^T K\underline{x}_e + \underline{x}_e^T\dot{K}\underline{x}_e + \underline{x}_e^T K\dot{\underline{x}}_e] + \frac{1}{2}\int_0^{t_{la}}\int_0^{t_{la}}[\frac{\partial w^T(t,\, l_1)}{\partial t}K_w(t,\, l_1,\, l_2)w(t,\, l_2) \\
&+ w^T(t,\, l_1)\frac{\partial K_w(t,l_1,l_2)}{\partial t}w(t,l_2) + w^T(t,\, l_1)K_w(t,\, l_1,\, l_2)\frac{\partial w(t,\, l_2)}{\partial t}]\, dl_1dl_2 \\
&+ \frac{1}{2}[\frac{\partial w^T(t+t_{la})}{\partial t}K_d(t)w(t+t_{la}) + w^T(t+t_{la})\dot{K}_d(t)w(t+t_{la}) + w^T(t+t_{la})K_d(t)\frac{\partial w(t+t_{la})}{\partial t}] \\
&+ \dot{\underline{x}}_e^T(t)\int_0^{t_{la}} F_1(t,\, l)w(t,\, l)dl + \underline{x}_e^T(t)[\int_0^{t_{la}}\frac{\partial F_1(t,\, l)}{\partial t}w(t,\, l) + F_1(t,\, l)\frac{\partial w(t,\, l)}{\partial t}]dl \\
&+ \dot{\underline{x}}_e^T(t)F_2(t)w(t+t_{la}) + \underline{x}_e^T(t)\dot{F}_2(t)w(t+t_{la}) + \underline{x}_e^T(t)F_2(t)\frac{\partial w(t+t_{la})}{\partial t}
\end{aligned}
\tag{A.2}
$$

And the partial derivative of J^* with respect to $\underline{x}_e$ is:

$$
\frac{\partial J^*}{\partial \underline{x}_e} = \underline{x}_e^T(t)K(t) + \int_0^{t_{la}} w^T(t,\, l)F_1^T(t,\, l)dl + w^T(t+t_{la})F_2^T(t) \tag{A.3}
$$

The optimal control signal $\delta_{opt}(t)$ can then be obtained by substituting Eqs.(A.3) and (14) into (15):

$$
\delta_{opt}(t) = -R^{-1}B_e^T[K(t)\underline{x}_e(t) + \int_0^{t_{la}} F_1(t,l)w(t,l)dl + F_2(t)w(t+t_{la})] \tag{A.4}
$$

Substitute (A.2) and (9) into (13), and note (A.4) and the following equations:

$$
\begin{aligned}
&\int_0^{t_{la}}\int_0^{t_{la}}\frac{\partial w^T(t,l_1)}{\partial t}K_w(t,l_1,l_2)w(t,l_2)dl_1dl_2 \\
&= \int_0^{t_{la}}\int_0^{t_{la}}\frac{\partial w^T(t,l_1)}{\partial l_1}K_w(t,l_1,l_2)w(t,l_2)dl_1dl_2 \\
&= \int_0^{t_{la}}[w^T(t,l_1)K_w(t,l_1,l_2)w(t,l_2)]\Big|_{l_1=0}^{l_1=t_{la}}dl_2 - \int_0^{t_{la}}\int_0^{t_{la}} w^T(t,l_1)\frac{\partial K_w(t,l_1,l_2)}{\partial l_1}w(t,l_2)\, dl_1dl_2 \\
&= \int_0^{t_{la}}[w^T(t,t_{la})K_w(t,t_{la},l)w(t,l) - w^T(t,0)K_w(t,0,l)w(t,l)]dl - \int_0^{t_{la}}\int_0^{t_{la}} w^T(t,l_1)\frac{\partial K_w(t,l_1,l_2)}{\partial l_1}w(t,l_2)\, dl_1dl_2
\end{aligned}
\tag{A.5}
$$

and

$$\int_0^{t_{la}}\int_0^{t_{la}} w^T(t,l_1)K_w(t,l_1,l_2)\frac{\partial w(t,l_2)}{\partial t}dl_1dl_2$$

$$= \int_0^{t_{la}}\int_0^{t_{la}} w^T(t,l_1)K_w(t,l_1,l_2)\frac{\partial w(t,l_2)}{\partial l_2}dl_1dl_2$$

$$= \int_0^{t_{la}}[w^T(t,l_1)K_w(t,l_1,l_2)w(t,l_2)]|_{l_2=0}^{l_2=t_{la}}dl_1 - \int_0^{t_{la}}\int_0^{t_{la}} w^T(t,l_1)\frac{\partial K_w(t,l_1,l_2)}{\partial l_2}w(t,l_2)\,dl_2dl_1$$

$$= \int_0^{t_{la}}[w^T(t,l)K_w(t,l,t_{la})w(t,t_{la}) - w^T(t,l)K_w(t,l,0)w(t,0)]dl - \int_0^{t_{la}}\int_0^{t_{la}} w^T(t,l_1)\frac{\partial K_w(t,l_1,l_2)}{\partial l_2}w(t,l_2)\,dl_2dl_1 \tag{A.6}$$

We obtain the following equation:

$$\begin{aligned}
\mathbf{o} = {} & \frac{1}{2}\underline{x}_e^TA_e^TK\underline{x}_e^T - \frac{1}{2}[\underline{x}_e^TKB_eR^{-1} + \int_0^{t_{la}} w^T(t,l)F_1^T(t,l)dlB_eR^{-1} + w^T(t+t_{la})F_2^T(t)B_eR^{-1}]B_e^TK\underline{x}_e \\
& + \frac{1}{2}w^TD_e^TK\underline{x}_e + \frac{1}{2}\underline{x}_e^T\dot{K}\underline{x}_e + \frac{1}{2}\underline{x}_e^TKA_e\underline{x}_e - \frac{1}{2}\underline{x}_e^TKB_eR^{-1}B_e^TK\underline{x}_e - \frac{1}{2}\underline{x}_e^TKB_eR^{-1}B_e^T\int_0^{t_{la}}F_1(t,l)w(t,l)dl \\
& - \frac{1}{2}\underline{x}_e^TKB_eR^{-1}B_e^TF_2(t)w(t+t_{la}) + \frac{1}{2}\underline{x}_e^TKD_ew \\
& + \frac{1}{2}w^T(t,t_{la})\int_0^{t_{la}}K_w(t,t_{la},l)w(t,l)dl - \frac{1}{2}w^T(t)\int_0^{t_{la}}K_w(t,0,l)w(t,l)dl \\
& + \frac{1}{2}\int_0^{t_{la}}\int_0^{t_{la}} w^T(t,l_1)[\frac{\partial K_w(t,l_1,l_2)}{\partial t} - \frac{\partial K_w(t,l_1,l_2)}{\partial l_1} - \frac{\partial K_w(t,l_1,l_2)}{\partial l_2}]w(t,l_2)dl_1dl_2 \\
& + \frac{1}{2}\int_0^{t_{la}} w^T(t,l)K_w(t,l,t_{la})dlw(t,t_{la}) - \frac{1}{2}\int_0^{t_{la}} w^T(t,l)K_w(t,l,0)dlw(t) + \frac{1}{2}\frac{\partial w^T(t+t_{la})}{\partial t}K_d(t)w(t+t_{la}) \\
& + \frac{1}{2}w^T(t+t_{la})\dot{K}_d(t)w(t+t_{la}) + \frac{1}{2}w^T(t+t_{la})K_d(t)\frac{\partial w(t+t_{la})}{\partial t} + \underline{x}_e^TA_e^T\int_0^{t_{la}}F_1(t,l)w(t,l)dl \\
& - [\underline{x}_e^TKB_eR^{-1} + \int_0^{t_{la}} w^T(t,l)F_1^T(t,l)dlB_eR^{-1} + w^T(t+t_{la})F_2^T(t)B_eR^{-1}]B_e^T\int_0^{t_{la}}F_1(t,l)w(t,l)dl \\
& + w^TD_e^T\int_0^{t_{la}}F_1(t,l)w(t,l)dl + \underline{x}_e^T\int_0^{t_{la}}[\frac{\partial F_1(t,l)}{\partial t} - \frac{\partial F_1(t,l)}{\partial l}]w(t,l)dl \\
& + \underline{x}_e^TF_1(t,t_{la})w(t,t_{la}) - \underline{x}_e^TF_1(t,0)w + \underline{x}_e^TA_e^TF_2(t)w(t+t_{la}) + w^TD_e^TF_2(t)w(t+t_{la}) \\
& - [\underline{x}_e^TKB_eR^{-1} + \int_0^{t_{la}} w^T(t,l)F_1^T(t,l)dlB_eR^{-1} + w^T(t+t_{la})F_2^T(t)B_eR^{-1}]B_e^TF_2(t)w(t+t_{la}) \\
& + \underline{x}_e^T\dot{F}_2(t)w(t+t_{la}) + \underline{x}_e^TF_2(t)\frac{\partial w(t+t_{la})}{\partial t} + \frac{1}{2}\underline{x}_e^TQ\underline{x}_e \\
& + \frac{1}{2}[\underline{x}_e^TKB_eR^{-1} + \int_0^{t_{la}} w^T(t,l)F_1^T(t,l)dlB_eR^{-1} + w^T(t+t_{la})F_e^T(t)B_eR^{-1}]R[R^{-1}B_e^TK\underline{x}_e \\
& + R^{-1}B_e^T\int_0^{t_{la}}F_1(t,l)w(t,l)dl + R^{-1}B_e^TF_2(t)w(t+t_{la})]
\end{aligned} \tag{A.7}$$

Grouping similar terms in Eq.(A.7), we obtain Eqs.(19)-(23).